AN OVERVIEW OF THE NASA FLYING TEST PLATFORM RESEARCH

K.B. Lim*, J-Y. Shin†, E.G. Cooper‡, D.D. Moerder§, T.H. Khong¶, M.F. Smith‖
NASA Langley Research Center
Hampton, Virginia, USA 23681

Abstract

A methodology for improving attitude stability and control for low-speed and hovering air vehicle is under development. In addition to aerodynamically induced control forces such as vector thrusting, the new approach exploits the use of bias momenta and torque actuators, similar to a class of spacecraft system, for its guidance and control needs. This approach will be validated on a free-flying research platform under development at NASA Langley Research Center. More broadly, this platform also serves as an in-house testbed for research in new technologies aimed at improving guidance and control of a Vertical Take-Off and Landing (VTOL) vehicle.

1 Research Motivation

This paper gives an overview of the ongoing research in precision guidance and robust control based on the NASA Flying Test Platform (NFTP) research vehicle currently under development at NASA Langley Research Center. The research is motivated by core GN&C objectives that include optimal guidance and navigation, and robust attitude and position stabilization under uncertain exogenous disturbances and model variations. A key goal of this research is to investigate novel technologies to improve attitude stability particularly during hovering or at low airspeed flight wherein conventional control effectors become ineffective. This particular need arises from current limitations in attitude stabilization performance for vector-thrusted air vehicles such as Osprey, Harrier VTOL, and for helicopters with sling loads. The basic and common limitation in the above control problem appears to be a lack of an accurate dynamical model suited for response prediction and controller design to attain precision and reliable performance under unsteady aerodynamics. In retrospect, this apparent performance limitation in the use of a vector-thrusting approach for dynamical stabilization of the vehicle is not surprising since stability is fundamentally an unsteady aerodynamics phenomenon. This phenomenon is the current limiting factor in predicting loads and responses on the vehicle (see for example, [1], [2]), which are necessary ingredients for robust and precise stabilizing feedback control.

*Senior Research Engineer, Guidance and Controls Branch, k.b.lim@larc.nasa.gov
†Staff Scientist, NIA, j.y.shin@larc.nasa.gov
‡Senior Research Engineer, Systems Integration Branch, e.g.cooper@larc.nasa.gov
§Senior Research Engineer, Guidance and Controls Branch, d.d.moerder@larc.nasa.gov
¶Research Engineer, Guidance and Controls Branch, t.h.khong@larc.nasa.gov
‖Technician, Guidance and Controls Branch, m.f.smith@larc.nasa.gov

2 Test Platform Description

2.1 System Configuration

Figure 1 shows the NFTP system, which consists of a square rigid platform levitated and propelled by a set of four battery-powered ducted fans each with a pair of control vanes. The vehicle employs a sensing system that fuses Inertial Measurement Unit (IMU) sensors and an optically based 6-DOF target tracking inertial position/attitude sensing system. The rigid platform is about 1.2 meters wide and weighs about 12 kg. The NFTP is a free flying vehicle designed to fly within a flight envelope box which is approximately 5 meters wide, indoors. Figure 2 is a schematic of the hardware architecture and major components for the basic NFTP system. The PC104 is used as the onboard flight control computer, which will implement an inner-loop controller for stability augmentation and has the capability of a wireless datalink to a ground control computer. A dSPACE system is used as the ground computer whose primary function is guidance from an operator, data logging, and communication with a vision system which tracks the flying vehicle. The flight control system will be capable of using all sensor measurements which include inertial measure-

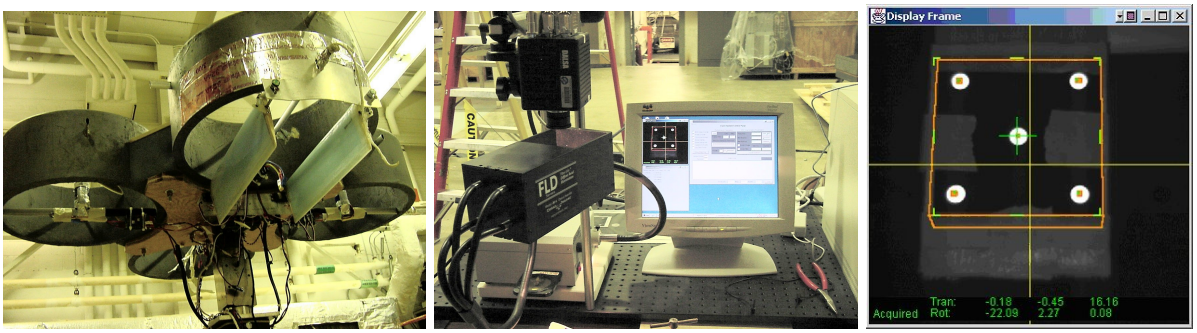

Figure 1: NASA Flying Test Platform (NFTP).

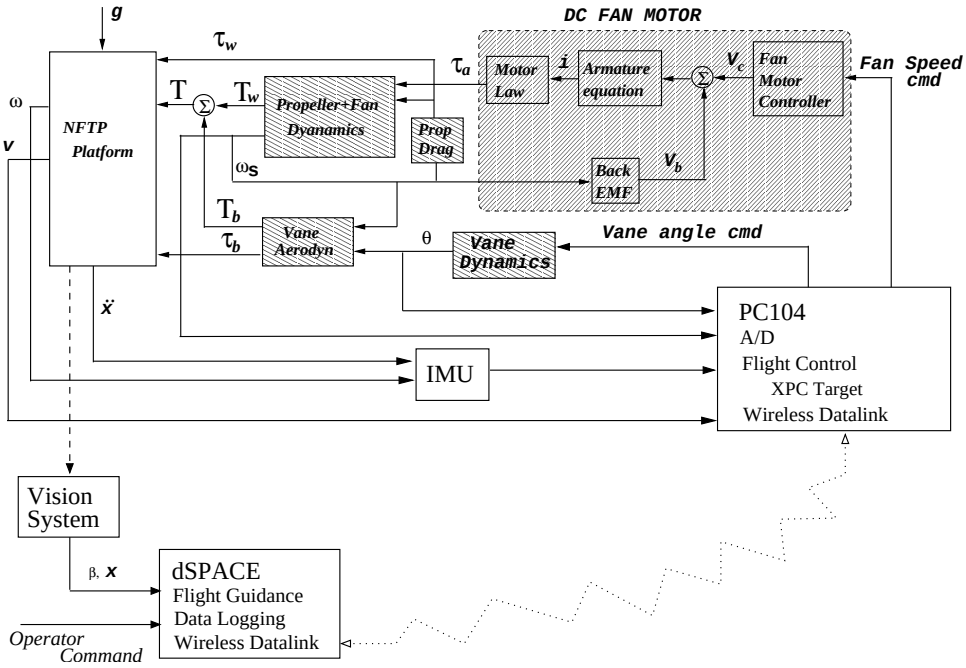

Figure 2: Basic NFTP component and hardware architecture.

ments from the IMU, fan speeds, vane angles, and the inertial position and attitude corrections from a ground based vision system.

The NFTP is specifically designed to facilitate research in precision guidance and robust control for the class of VTOL vehicles, especially during hovering or at low air speeds. As a testbed, the NFTP provides realism, focus, and the flexibility necessary in any research to develop new technology. Specifically, it provides performance targets (for example as a flying platform in a search and rescue scenario), hardware limitations (for example, due to saturation, hysterisis, control effectiveness), realistic unsteady aerodynamics, and real time flight control operational limitations. The testbed will also help clarify technology show-stoppers and define the state-of-the-art in vehicle control at low speeds and hovering, which many of today's air vehicles face daily. The testbed will also help motivate and illuminate robustness issues in trajectory and attitude control problems, which is mainly caused by the limitation in dynamical modeling of the controlled vehicle. Finally, the testbed provides a common focus for research between disparate guidance and navigation research and robust control disciplines.

2.2 Analytical Modeling of Rigid Platform with Vectored Fans

A Newton-Euler formulation is used to derive the equations of motion for the basic NFTP. In particular the notation and formulation in [7] is used and

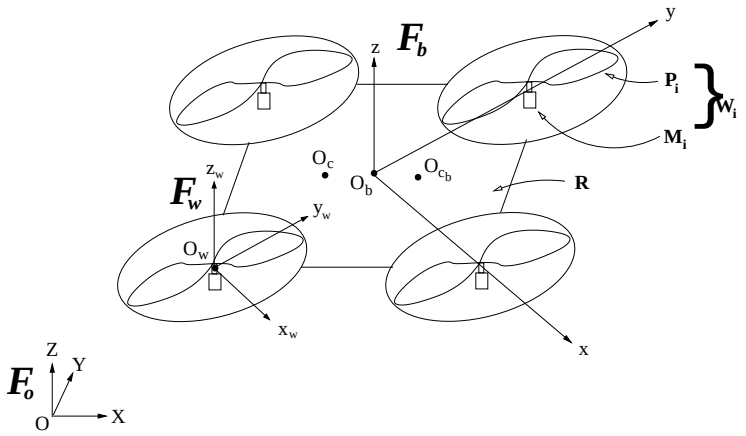

R	NFTP system excluding spinning bodies
W_i	i-th Propeller(P_i)-Motor(M_i) unit
XY	floor plane
O_b	origin of platform fixed axes, (x, y, z)
O_w	origin of fan axes, (x_w, y_w, z_w)
O_c	c/m of NFTP system
O_{c_b}	c/m of R

Figure 3: Schematic of NFTP.

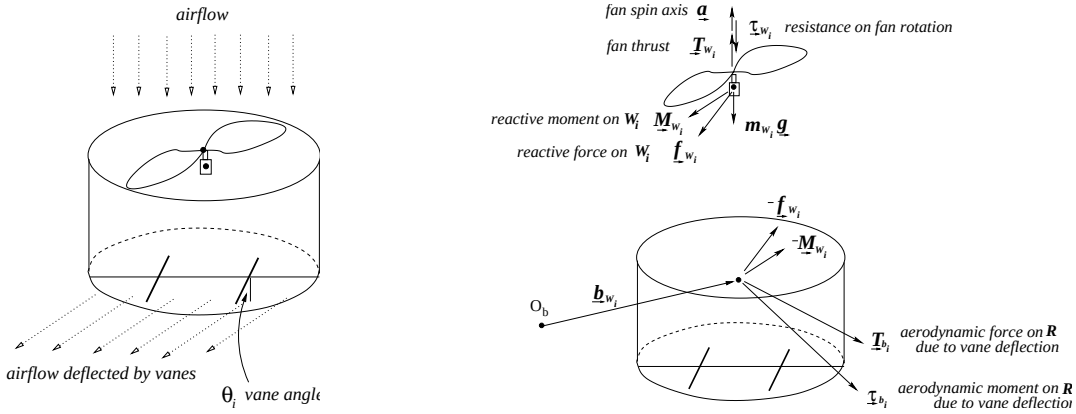

Figure 4: Schematic of forces and moments during fan rotation and vane deflection.

extended to include multiple spinning bodies with vane rotational motion for active flow deflection. Figure 3 shows a schematic of the NFTP describing its main components. The degrees of freedom for the basic NFTP model include the following: 3 positions (O_b relative to O), 3 rotations of R (relative to F_o), 4 rotations of fan (relative to F_b), and 4 pairs of rotating vanes (relative to F_w), for a total of 14 degrees of freedom. Figure 4 illustrates the forces and moments acting on the spinning propeller and motor assembly, W_i $(= P_i + M_i)$, and on the platform, R, due to fan rotation and vane deflection. The rotating fan produces airflow through the duct thereby generating propulsive thrust, $\underset{\rightarrow}{T}_{w_i}(\omega_{s_i}, \text{propeller aerodynamics})$, and rotational aerodynamic resistance, $\underset{\rightarrow}{\tau}_{w_i}(\omega_{s_i}, \text{propeller aerodynamics})$, along the fan spin axis, $\underset{\rightarrow}{a}_i$. Since the spin axis is fixed in R, these forces and moments along with the tendency of the motion in R results in internal reactive forces and moments, $\underset{\rightarrow}{f}_{w_i}$ (dynamics of W_i and R), and $\underset{\rightarrow}{M}_{w_i}$(dynamics of W_i and R), acting on W_i. Finally, the deflection of the downstream flow by the vanes produces forces and moments, $\underset{\rightarrow}{T}_{b_i}(\omega_{s_i}, \theta_i, \text{vane aerodynamics})$, and $\underset{\rightarrow}{\tau}_{b_i}(\omega_{s_i}, \theta_i, \text{vane aerodynamics})$, on R. The motion equations are given as follows:

$$\underset{\rightarrow}{\dot{p}} = m\,\underset{\rightarrow}{g} + \sum_{i=1}^{4}(\underset{\rightarrow}{T}_{b_i} + \underset{\rightarrow}{T}_{W_i}) \tag{1}$$

$$\underset{\rightarrow}{\dot{h}} = -\underset{\rightarrow}{v} \times \underset{\rightarrow}{p} + \underset{\rightarrow}{c} \times \underset{\rightarrow}{g} + \sum_{i=1}^{4} \underset{\rightarrow}{b}_{W_i} \times \underset{\rightarrow}{T}_{W_i} + \tau_{W_i}\,\underset{\rightarrow}{a}_i + \underset{\rightarrow}{b}_{W_i} \times \underset{\rightarrow}{T}_{b_i} + \underset{\rightarrow}{\tau}_{b_i} \tag{2}$$

$$\dot{h}_{a_i} = \underset{\rightarrow}{a}_i \cdot \underset{\rightarrow}{M}_{W_i} + \tau_{W_i} \tag{3}$$

and the linear and angular momenta are given as

$$\underset{\rightarrow}{p} = m\,\underset{\rightarrow}{v} + \underset{\rightarrow}{\omega} \times \underset{\rightarrow}{c} \tag{4}$$

$$\underset{\rightarrow}{h} = \underset{\rightarrow}{c} \times \underset{\rightarrow}{v} + \underset{\rightarrow}{J} \cdot \underset{\rightarrow}{\omega} + \sum_{i=1}^{4}(I^a_{M_i} + \frac{1}{\gamma} I^a_{P_i})\omega_{s_i}\,\underset{\rightarrow}{a}_i \tag{5}$$

$$h_{a_i} = (I^a_{M_i} + I^a_{P_i})\,\underset{\rightarrow}{a}_i \cdot \underset{\rightarrow}{\omega} + (I^a_{M_i} + \frac{1}{\gamma} I^a_{P_i})\omega_{s_i} \tag{6}$$

where $i = 1, \ldots, 4$ and $\underrightarrow{p}$ denotes the momentum of the entire system, $S := R + \sum_{i=1}^{4} W_i$, with mass, m, while $\underrightarrow{v}$ denotes the inertial velocity of the origin of platform fixed axes F_b whose inertial angular velocity is $\underrightarrow{\omega}$, and $\underrightarrow{c}$ denotes the first moment of inertia of the entire system relative to O_b. Vector $\underrightarrow{h}$ denotes the angular momentum of the entire system about O_b. h_{a_i} denotes the component along the spin axis $\underrightarrow{a}_i$ of the angular momentum of W_i about its center of mass. ω_{s_i} denotes the angular velocity of ith motor, M_i, relative to F_b frame. In the initial flight experiments, where separate bias momentum wheels nor CMGs will not be available, the spinning of the four fans in the same direction will be the only source for generating and maintaining bias momenta for the overall system. The corresponding rotational inertia, $I^a_{M_i} + \frac{1}{\gamma} I^a_{P_i}$, will be appropriately sized based on parametric studies, for the goal of making the bias momenta effects sufficiently useful for pointing stability.

After selecting appropriate coordinate system to describe vector elements, the governing dynamic equations in (1) to (3) can be rewritten in scalar form for computation, while the kinematic equations are written as

$$\dot{\beta} = \begin{bmatrix} 0 & -\omega_1 & -\omega_2 & -\omega_3 \\ \omega_1 & 0 & \omega_3 & -\omega_2 \\ \omega_2 & -\omega_3 & 0 & \omega_1 \\ \omega_3 & \omega_2 & -\omega_1 & 0 \end{bmatrix} \beta, \ \beta^T \beta = 1 \quad (7)$$

$$\dot{\xi} = C(\beta)^T v \quad (8)$$

where ω_1, ω_2, and ω_3 are components of $\underrightarrow{\omega}$ in F_b frame while ξ denotes the position of O_b in F_o frame, and $\beta \in \mathcal{R}^4$ denotes quarternion for attitude parameterization. The forces and moments generated by the fans amd vanes depend on states and commands, as follows: $T_{W_i}(\omega_{s_i}) \in \mathcal{R}$, $T_{b_i}(\omega_{s_i}, \theta_i) \in \mathcal{R}^{3\times 1}$, $\tau_{a_i}(\omega_{s_i}, \omega^{cmd}_{s_i}) \in \mathcal{R}$, $\tau_{W_i}(\omega_{s_i}) \in \mathcal{R}$, $\tau_{b_i}(\omega_{s_i}, \theta_i) \in \mathcal{R}^{3\times 1}$, $\tau_{a_{T_i}}(\Omega_{s_i}, \Omega^{cmd}_{s_i}) \in \mathcal{R}$. By denoting the following state and input variables,

$$x := \begin{Bmatrix} p \\ h \\ h_a \\ \beta \\ \xi \end{Bmatrix} \quad u := \begin{Bmatrix} \omega_s \\ \theta \end{Bmatrix}$$

and noting that the machine vision system directly sense the inertial orientation of the body frame F_b denoted by Euler parameters β, and the inertial position of O_b denoted by ξ, the governing set of equations can be written symbolically as

$$\begin{aligned} \dot{x} &= f(x, u, K) + \nu_x \\ y &= g(x, u, K) + \nu_y \end{aligned} \quad (9)$$

where the output vector is given by

$$g(x, u, K) := \begin{bmatrix} 0 & 0 & 0 & I & 0 \\ 0 & 0 & 0 & 0 & I \end{bmatrix} x$$

The set of scalars K represent constant parameters while $\nu := [\nu_x, \nu_y]$ denotes process and output noises. The functions f and g are clearly differentiable. Note that the momenta components of the state, (p, h, h_a), are linearly related to the corresponding velocities, (v, ω, ω_s), as given by the relationship in equations (4) to (6).

2.3 Perturbed Dynamics about Trim

Precluding rapid maneuvers or any motions with high accelerations for the NFTP platform, the subset of motions which are near hovering or at low airspeeds can be viewed as motions near a trim point. This means that we can approximate and simplify the nonlinear dynamical equations in 9 by linearizing it about a physically significant reference trajectory (x_o, u_o), namely, any point in an equilibrium manifold. Specifically, we are interested in equilibrium trim in all six degrees of freedom of the platform and in all four fan's rotational motion, i.e., $\dot{x}_o = f(x_o, u_o, K) = 0$. Additionally, we are interested in the subset of trim conditions with zero platform angular rate, namely $\omega = 0$. It turns out that for a given platform attitude, the trim fan speeds and the corresponding vane angles, denoted by $u_o^T = (\omega_{s_o}^T, \theta_o^T)$, must satisfy the following conditions:

$$[A + B \cdot \mathrm{diag}(\theta_o) + C \cdot \mathrm{diag}(\theta_o)^2] T_W(\omega_{s_o}) + F = 0_{6\times 1} \quad (10)$$

while A, B, C, F are model parameters that capture the geometry, mass properties, fan and vane aerodyanmics, and the desired trim platform attitude. By denoting $u := u_o + \delta u$, $y := y_o + \delta y$, $x := x_o + \delta x$, we can linearize equation 9 about the reference trajectory (x_o, u_o) as

$$\delta \dot{x} = A(x_o, u_o, K)\delta x + B(x_o, u_o, K)\delta u + \ldots \quad (11)$$

$$\delta y = C(x_o, u_o, K)\delta x + D(x_o, u_o, K)\delta u + \ldots \quad (12)$$

where $A(x_o, u_o, K) := \frac{\partial f}{\partial x}(x_o, u_o)$, $B(x_o, u_o, K) := \frac{\partial f}{\partial u}(x_o, u_o)$, $C(x_o, u_o, K) := \frac{\partial g}{\partial x}(x_o, u_o)$, $D(x_o, u_o, K) := \frac{\partial g}{\partial u}(x_o, u_o)$.

2.4 Identification of Model Parameters

The end goals for generating a mathematical model are for the prediction, analysis, and controller design of the full NFTP system. In this modeling effort, we

incorporate static and dynamic relationships from first principles, albeit an oversimplification, and use experimental data to estimate physical parameters of the model and characterize the uncertainties.

Both the reference trajectory equations (trimmed or not) and the linearized perturbed equations depend on a set of model parameters, denoted earlier as K, that need to be identified and validated, to be of practical use. Obviously for trim conditions, bench tests can be used to determine a subset of these model parameters. On the other hand, the perturbed motion has the form of linear time-varying equations. If the trim inputs and states as given by (x_o, u_o) are slowly time varying (which would likely be true for near hovering and at low airspeed conditions), and measured fully in real time, then these slowly time varying inputs and states can be considered as known parameters or gains that can be "scheduled" in time for feedback control. Hence this perturbed motion conforms to a linear parameter varying (LPV) model with the benefit of an abundance of control theory that supports a well founded framework for feedback control analysis and design, see for example, [8, 9, 10, 11, 12, 13]. On the other hand, although a substantial body of control theory for LPV systems exists today, there appears to be a lack of methodical modeling techniques that can be used for real applications. Indeed, only a handful of published work is available in the open literature on modeling and identification of LPV systems [14, 15, 16, 17] and even fewer show results based on experimental data.

In this research, a first principle analytic model of a single ducted fan is developed under various simplifying assumptions including ideal airflow inside the duct and over the vanes, dynamics of the electric brush-less fan motor, fan rotational drag, and simplifying assumptions on fan and vane configurations and their kinematics. This functional form of the model with various physical coefficients are used in a series of static and dynamic bench tests. In these series of experiments designed to characterize the dynamics of a single ducted fan, the duct housing is rigidly connected to the non-rotating component of the motor which is itself attached to the top of a 6-DOF load cell and supported by a semi-rigid pole fixed to the laboratory floor.

The set of unknown model parameters that needs to be determined include: fan thrust coefficients, fan rotational drag coefficients, van deflection force and moment coefficients, back electromagnetic force (EMF) resistance coefficients, moment of inertias of the rotating motor components including propellers, and parameters that describe the effect of aero load on vane deflection angle command. In this study, we propose fitting an LPV model of the perturbed dynamics, given by $A(x_o, u_o, K)$, $B(x_o, u_o, K)$, $C(x_o, u_o, K)$, $D(x_o, u_o, K)$, by optimizing the unknown but constant parameters, K, such that the fitted LPV model will optimally match a set of LTI frequency response models over discrete set of gain scheduled parameters.

2.5 Attitude Control Approach

A highly unconventional approach we are investigating, in our attempt to improve attitude stability and control for a hovering or low airspeed vehicle, consists of the following key elements: (1) use of bias momenta to improve inherent pointing stability, (2) use of high precision torque actuators such as reaction wheels or Control Moment Gyros (CMG) for feedback stabilization, and (3) use of aerodynamically induced control forces (including vector thrusting or differential air-ducting) for maintaining trim conditions. The first two elements involve adapting flight proven spacecraft attitude control technologies to an air vehicle. For element one, the use of bias momenta to provide spin/gyroscopic stability for fine pointing is well known for the class of dual-spin space vehicles (see for example [3], [4], [5]). In element two, the use of high precision torque actuators such as CMGs, in lieu of aerodynamically induced control forces, is highly unconventional although this is a well proven technology for the attitude control of a significant class of space vehicles [3]. For the third element, the use of aerodynamically induced control forces for trimming is common practice but what it should not do is significant - it should not be in the attitude stabilization inner-loop.

Currently, the only set of air vehicles that inadvertently appears to take advantage of bias momenta for pointing stability is the helicopter with a single main rotor. However, elements two and three are not incorporated for this class of helicopters [6]. In essence, a dual-spin vehicle incorporating the above three elements will inherently possess pointing stability, which is well suited for the hovering requirement, and any perturbations can be reliably compensated using precision CMG type actuators. In addition, the inherent "stiffness" due to bias momenta will also mitigate attitude perturbations and response speeds, which makes the feedback control problem more promising. By keeping the unsteady aerodynamics out of the stability augmentating closed inner-loop, the stability analysis, control design, and closed loop

simulation will in principle be simpler and more realistic since the unsteady aerodynamics can then be considered an unknown but bounded exogenous disturbances. These complex unsteady aerodynamic effects modeled as exogenous disturbances can then be methodically addressed by well established disturbance rejection control techniques.

3 Sample Simulation Results

In this section, nonlinear simulations of NFTP are presented to demonstrate the concept of using bias momentum to improve inherent (open loop) attitude stability. For the baseline NFTP system considered currently, the bias momentum is introduced by rotating all four fans in the same direction, in contrast to conventional applications where propellers are counter-rotated to cancel gyroscopic effects. To demonstrate the inherent attitude stability due to the presence of bias momentum, we simulate the responses due to perturbations caused by (1) a set of unbalanced motor torques, and (2) gust. For each of the two simulation scenarios we will show the results of counter-rotating propellers as well as same-direction rotating propellers.

In the following sample simulations, we make the following simplifying assumptions which will likely not change the effects of bias momemtum and attitude stability: (i) exclude vane effects, (ii) exclude all resistance on fan motion having spin axis $\underrightarrow{a}_i := \hat{z}$, (iii) exclude fan motor dynamics, (iv) fan thrust $\underrightarrow{T}_{W_i} := T_{max}\left\{\frac{\omega_{s_i}}{\omega_{s_{i_{max}}}}\right\}^2 \hat{z}$ where T_{max} and $\omega_{s_{i_{max}}}$ are maximum thrust and motor speed, respectively, and $\hat{z}$ is a unit vector in the F_b frame.

3.1 Unbalanced motor torque

This simulation is comprised of a vertical maneuver (ascent and descent) resulting from the motor control torque schedules defined in Tables 1 and 2. A slightly unbalanced control torque is introduced for counter and same-direction rotating fans, respectively. Figure 5 shows the NFTP attitude response according to the pre-defined motor control input for cases: Case with fan rotation in Counter Direction cd_{opl} (resulting in zero bias momentum), case with fan rotation in Same Direction sd_{opl} (resulting in bias momentum), and case with fan rotation in Same Direction with feedback control sd_{clp}. The feedback control is $u = -k\omega_3$, where ω_3 is the component of the NFTP inertial angular velocity in the body z-axis. It is observed in

M_{W_1} (N-m)	M_{W_2}	M_{W_3}	M_{W_4}	Time (sec)
0.05	0.05	-0.05	-0.05	$0.5 \leq t \leq 8$
-0.059	- 0.06,	0.06,	0.06	$8 < t < 18$
0	0	0	0	$18 \leq t$

Table 1: Unbalanced motor control torque for counter rotating fans.

M_{W_1} (N-m)	M_{W_2}	M_{W_3}	M_{W_4}	Time (sec)
0.05	0.05	0.05	0.05	$0.5 \leq t \leq 8$
-0.059	- 0.06,	-0.06,	-0.06	$8 < t < 18$
0	0	0	0	$18 \leq t$

Table 2: Unbalanced motor control torque for same directional rotating fans.

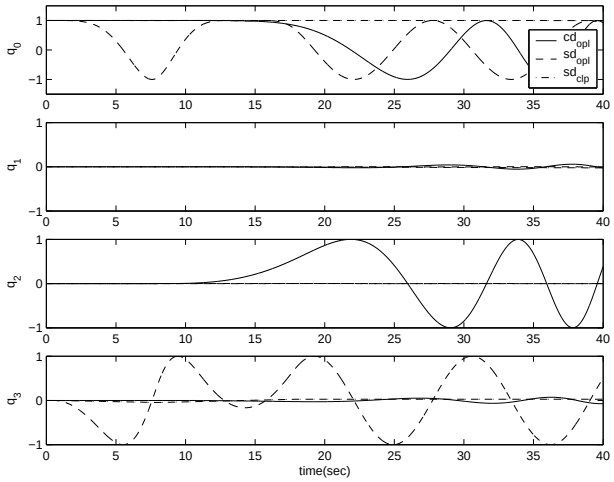

Figure 5: Vehicle attitude response due to unbalanced torque.

Figure 5 that the vehicle attitude is significantly tilted due to unbalanced thrust moment for the cd_{opl} case, the vehicle body counter rotates due to large net internal motor torque for the sd_{opl} case, and the vehicle attitude remains stationary for the sd_{clp} case because the feedback control law compensates for unbalanced net internal motor torque. The feedback control signals for each fan are shown in Figure 6. It shows that the small thrust of about $0.1N$ (cf. net thrust of vehicle to support its weight is about $120N$) compensates for unbalanced net internal motor torque for this simulation scenario.

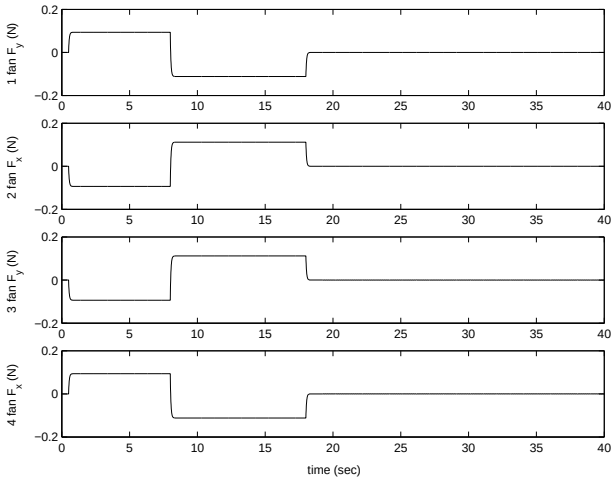

Figure 6: Feedback control signal in response to unbalanced thrust.

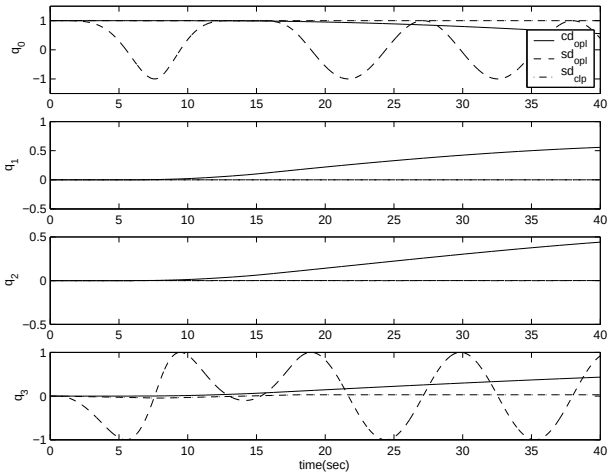

Figure 7: Vehicle attitude response to gust.

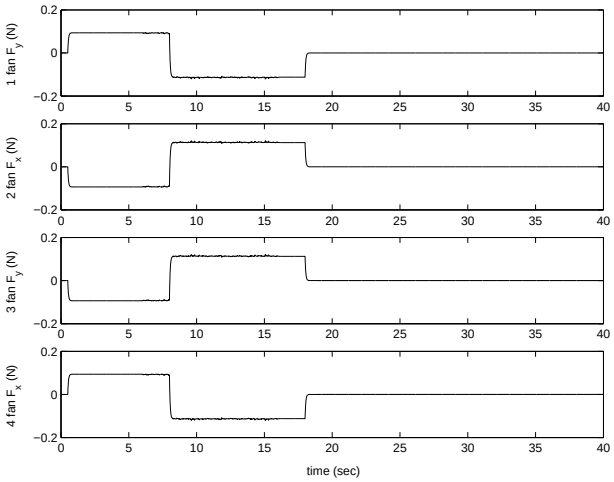

Figure 8: Feedback control signals to gust response.

3.2 Gust responses

With given gust velocity magnitude (V_g), gust effective force and torque on the NFTP are assumed as:

$$\begin{aligned} \underrightarrow{T}_{gust} &= C_{bi}(q)\underrightarrow{T}_{in} \\ \underrightarrow{\tau}_{gust} &= C_1\underrightarrow{T}_{gust} + \tau_{rand} \end{aligned}$$

where C_{bi} is a rotation matrix from inertial coordinates to body coordinates, C_1 is a constant matrix coefficient and τ_{rand} simulates an effective torque on the platform due to atmospheric turbulence. $\underrightarrow{T}_{in}$ is defined as gust force in inertial coordinates such that the force is a function of gust velocity and gust direction. The magnitude of the force $\underrightarrow{T}_{in}$ is defined as $0.5\rho V_g^2 S_{eff}$ where S_{eff} is effective area of the platform. Gust responses are simulated in Figure 7 for the above three cases: cd_{opl}, sd_{opl}, and sd_{clp}, under the assumption that gust velocity magnitude (V_g) is a normal distribution with mean 2 m/sec and σ of 5 m/sec. For the gust response cases, a perfectly balanced motor control torque for all cases are assumed. It is obvious from Figure 7 that the vehicle attitude is significantly tilted due to gust for cd_{opl} case. The bias momentum generated by same-direction rotating fans significantly stabilizes the vehicle attitude with the very simple feedback control law shown in Figure 8.

4 Conclusions

Viewing the NFTP as a rescue flying platform offers several advantages. This is because in a rescue scenario, it is inevitable that we need significant levels of robustness, reliability, safety, and precision in the flight control problem, for effective and safe operation. Important factors that one must accommodate include significant mass and inertia variations, and significant turbulence. The challenge is to attain precise control and predictable attitude stability while tolerating significant variations in the vehicle and disturbances. The NFTP testbed is well suited for laboratory simulation of the above factors.

There are many NFTP related activities currently underway. These include: configuration design and bench testing of real-time optical based inertial sensing system, sensor fusion with IMU sensor subsystem, characterization of ducted fan and vane dynamics based on first physical principle model aided with extensive single duct bench testing, independent measurements to characterize rotational inertias and fan

drag, integration of wireless telemetry system for control and data downlink, and safety issues related to free flying inside of laboratory. In addition, activities related to controller design and analysis, which are currently underway include: trim conditions based on arbitrary platform attitude hold, definition of control requirements and mission, performance and robustness metric development, controller synthesis and analysis, end-to-end simulation, and parametric study on spin stabilization. Preliminary and limited simulation results indicate that the bias momentum due to the same-direction rotating fans should significantly improve attitude stability under simulated perturbations due to imbalance motor torque or gust. In the near future, we plan to report detail and more conclusive results of our analysis, simulation, bench tests, and free flight experiments with the NFTP system.

References

[1] Gad-el-Hak, M., *Flow Control*, Cambridge University Press, Cambridge, UK, 2000.

[2] "Flow Control: Fundamentals and Practices," AIAA Professional Short Course, 22-23 June 2002, St. Louis, Missouri.

[3] *Spacecraft Attitude Determination and Control*, Ed. J.R. Wertz, Kluwer Academic Publishing, Boston, MA, v.73, 1995 (reprint).

[4] Junkins, J.L., and Turner, J.D., *Optimal Spacecraft Rotational Maneuvers*, Elsevier, Amsterdam, Netherlands, 1986.

[5] Wie, B., *Spacecraft Vehicle Dynamics and Control*, AIAA Education Series, AIAA, Inc., Reston, Virginia, 1998.

[6] Prouty, R.W., *Helicopter Aerodynamics*, Vols. I-III, PJS Publications Inc, Peoria, Ill, 1985-1993.

[7] Hughes, P.C., *Spacecraft Attitude Dynamics*, John Wiley & Sons, New York, 1986.

[8] Shamma, J. and Athans, M., "Guaranteed Properties of Gain Scheduled Control for Linear Parameter-Varying Plants," Vol. 35, No. 8, 1991, pp. 559–564.

[9] Apkarian, P. and Adams, R., "Advanced Gain-Scheduling Techniques for Uncertain Systems," *IEEE Transactions on Control Systems Technology*, Vol. 6, No. 1, 1998, pp. 21–32.

[10] Becker, G., *Quadratic Stability and Performance of Linear Parameter Dependent Systems*. PhD thesis, Department of Mechanical Engineering, University of California, Berkeley, 1993.

[11] Shin, J.-Y., *Worst-Case Analysis and Linear Parameter-Varying Gain-Scheduled Control of Aerospace Systems*. PhD thesis, Department of Aerospace Engineering and Mechanics, University of Minnesota, 2000.

[12] Shin, J.-Y., Balas, G.J., and Kaya, M.A., "Blending Methodology of Linear Parameter Varying Control Synthesis of F-16 Aircraft System," *Journal of Guidance, Control, and Dynamics*, Vol. 25, No. 6, 2002, pp. 1040–1048.

[13] Tan, W,, Packard, A,, and Balas, G., "Quasi-LPV Modeling and LPV Control of a Generic Missile," in *Proceedings of the American Control Conference*, (Chicago, IL), 2000, pp. 3692–3696, American Automatic Control Council, Evanston, IL.

[14] Nemani, M., Ravikanth, R., and Bamieh, B., "Identification of Linear Parametrically Varying Systems," in *IEEE Proceeding of the Conference on Decision and Control*, 1995, pp. 2990–2995.

[15] Lee, L. and Poolla K., "Identification of Linear Parameter-Varying Systems Using Nonlinear Programming," *Journal of Dynamic Systems, Measurement, and Control*, Vol. 121, No. 1, 1999, pp. 71–78.

[16] Bamieh, B. and Giarre, L., "Identification of Linear Parameter Varying Model," in *IEEE Proceeding of the Conference on Decision and Control*, 1999.

[17] Sznair, M., Mazzaro, C., and Inanc, T., "An LMI Approach to Control Oriented Identification of LPV Systems," in *Proceedings of the American Control Conference*, 2000, pp. 3682–3686.